energies

MDPI

Article

Performance of Corn Cob Combustion in a Low-Temperature Fluidized Bed

Rolandas Paulauskas [1,*], Marius Praspaliauskas [2], Ignas Ambrazevičius [1], Kęstutis Zakarauskas [1], Egidijus Lemanas [2], Justas Eimontas [1] and Nerijus Striūgas [1]

[1] Laboratory of Combustion Processes, Lithuanian Energy Institute, Breslaujos Str. 3, LT-44403 Kaunas, Lithuania; ignas.ambrazevicius@lei.lt (I.A.); kestutis.zakarauskas@lei.lt (K.Z.); justas.eimontas@lei.lt (J.E.); nerijus.striugas@lei.lt (N.S.)

[2] Laboratory of Heat-Equipment Research and Testing, Lithuanian Energy Institute, Breslaujos Str. 3, LT-44403 Kaunas, Lithuania; marius.praspaliauskas@lei.lt (M.P.); egidijus.lemanas@lei.lt (E.L.)

* Correspondence: rolandas.paulauskas@lei.lt; Tel.: +370-37-401830

Abstract: This study investigates the combustion of agricultural biomass rich in alkali elements in the fluidized bed. The experiments were performed with smashed corn cob in a 500 kW fluidized bed combustor which was designed for work under low bed temperatures (650–700 °C). During the experiments, the formed compounds from corn cob combustion were measured by sampling particulate matter, and mineral compositions were determined. Also, the temperature profile of the FBC was established. It was determined that the emissions of K and Na elements from the FBC increased from 4 to 7.3% and from 1.69 to 3%, respectively, changing the bed temperature from 650 to 700 °C. Though alkali emissions are reduced at a 650 °C bed temperature, CO emissions are higher by about 50% compared to the case of 700 °C. The addition of 3% of dolomite reduced the pollutant emissions and alkali emissions as well. Potassium content decreased by about 1% and 4%, respectively, at the bed temperatures of 650 °C and 700 °C. The NOx emissions were less than 300 mg/m^3 and did not exceed the limit for medium plants regarding DIRECTIVE (EU) 2015/2193. During extended experiments lasting 8 h, no agglomeration of the fluidized bed was observed. Moreover, the proposed configuration of the FBC and its operational parameters prove suitable for facilitating the efficient combustion of agricultural biomass.

Keywords: agro biomass; corn cob; fluidized bed; combustion; alkali; agglomeration; emissions

Citation: Paulauskas, R.; Praspaliauskas, M.; Ambrazevičius, I.; Zakarauskas, K.; Lemanas, E.; Eimontas, J.; Striūgas, N. Performance of Corn Cob Combustion in a Low-Temperature Fluidized Bed. *Energies* **2024**, *17*, 2196. https://doi.org/10.3390/en17092196

Academic Editor: Alberto Pettinau

Received: 22 March 2024
Revised: 23 April 2024
Accepted: 30 April 2024
Published: 3 May 2024

1. Introduction

Each EU member must reduce greenhouse gas emissions by 10 to 50% by 2030. Energy production from renewable energy sources (RES) will have to be increased in order to meet the tightened targets. Biomass is considered one of the main renewable energy sources to replace fossil fuels with the rapid development of agriculture, the use of agricultural biomass in energy has become extremely relevant [1,2] in low- and medium-power combustion plants.

Corn cobs, being the non-consumable post-harvest remnants of corn, contribute to a substantial volume of corn-related waste across the world each year [3]. Global production of corn cob residues is about 18% of the global corn production of about 797 million tons [4]. The EU's harvested production of grain maize and corn–cob mix weighed about 60 million tons per year. After minimal preparation and grinding, this agro-waste could be used in thermochemical processes, such as gasification or direct combustion, and produce a high amount of heat and electricity energy. That kind of fuel could increase independence from fossil fuels and decrease environmental pollution worldwide [5]. Despite this attractive characterization of corn cob, that kind of raw material fuel has some disadvantages related to chemical composition. Corn cob has completely different concentrations of potassium (K), calcium (Ca), phosphorus (P), sodium (Na), chlorine (Cl), sulfuric (S), and other chemical

elements compared to traditional wood biofuel. Agro-biomass is a specific material as a fuel due to different planting environments, harvesting seasons, and different fractions of agro-biomass [6]. The chemical composition of such fuel can differ significantly, i.e., Al, Ca, Fe, Mg, P, K, Si, Na, Ti, Zn, and Pb. Because of this, direct combustion causes difficult to control problems. The use of such fuel becomes completely unattractive for heat producers, although its quantities are quite significant. During combustion in moving-grate or fixed-grate furnaces becomes complicated due to the high concentration of Cl, S, and alkali metals (K and Na) in such biomass, deposits rapidly begin to accumulate on the combustion surfaces, as well as slag accumulation on heat exchangers and slag accumulation caused by silicate (Si) melt on water-cooled walls [7]. According to Shao et al. [8], potassium (K) evaporation from fuel starts from 650 °C, and the highest rates are reached at ~1000 °C. Other authors determined that at temperatures from 600 to 815 °C, evaporated potassium (K) reacts with chlorine (Cl) and forms potassium chloride (KCl), which participates in slagging and fouling and causes corrosive problems [9]. The formation of these compounds is treated as the initial stage of further aerosol formation [10]. Larger aerosol formations gradually form around K and Na sulphates and chlorides. If the amount of S and Cl in the fuel is lower, carbonates begin to form faster, and K and Na in the fuel are bound [11]. Volatile heavy metals, such as Zn and Pb, are also detected in aerosols. The concentrations of these elements in aerosols directly depend on the raw fuel used for burning (poor quality).

Fluidized bed boilers are a well-known technology and provide a number of advantages, like fuel flexibility, higher efficiency of heat and mass transfer, considerably low combustion temperatures (up to 800 °C), and lower pollutant emissions [12,13]. For example, municipal waste combustion was investigated in a two-stage fluidized bed combustor [14]. Low-temperature combustion of 400–800 °C was performed in the first stage, and it allowed the reduction of heavy metal concentrations from 16 to 82% in the flue gas. Another work showed promising results on phosphorus (P)- and potassium (K)-reduced emissions during the thermal conversion of the sewage sludge and wheat straw mixture in the fluidized bed at 750 °C [15,16]. Karel et al. [17] investigated conifer bark and eucalyptus cutting waste combustion in the fluidized bed at 600–800 °C and, by changing the air equivalence ratio, were able to achieve stable combustion without defluidization. Experiments with oat seeds and sunflower husks in a 75 MW circulating fluidized bed combustor revealed that the combustion at 750 °C neglects ash agglomeration in the bed, but slagging on the walls leads to more intense defluidization as pieces of slag drop to the bed [18]. Other studies [19,20] showed that agricultural biomass combustion in a low-temperature 600–650 °C fluidized bed could result in incomplete combustion and increased NOx, CO, and particulate matter (PM) emissions, which is related to the air equivalence ratio and volatile evaporation rate from fuel in the bed.

Using fuel additives that have varied chemical compositions is an effective strategy for lessening and offsetting the negative impacts observed in combustion processes. Such additives aid in the establishment of new chemical bonds, thereby converting problematic elements responsible for ash formation into stable materials possessing high melting points [21,22]. Since the use of fuel additives is related to economic factors, it is very important to determine what amount of additive would be sufficient to solve the desired problems. Calculating the required quantity of fuel additive often relies on stoichiometric calculations, indicating the necessity for more laboratory investigations to elucidate the phenomena in true scenarios. Furthermore, it is essential to find further fuel additives that boast high stability and reactivity and are economically feasible [22]. The most appropriate option would be if the fuel additive was a waste production material, the price of which being low and the available quantities being large. Using additives and combined fuel aims to change the composition of the raw material and additionally reduce the share of volatile alkaline elements in the fuel used. Research has shown that blending low-quality fuel with additives can lead to a decrease in the formation of solid particles and other combustion by-products, such as NOx, SO_2, and HCl, during the combustion

process [23]. During gasification, dolomite undergoes calcination to yield CaO, which acts to prevent agglomeration by favoring the formation of K_2CO_3 over K_2OnSiO_2 [24]. This effect was observed in gasification processes occurring at temperatures ranging from 650 to 850 °C, which were associated with optimal heating values, gas yields, carbon conversion rates, and cold gas efficiencies. The use of dolomite as an additive resulted in reduced agglomerate formation up to 850 °C, demonstrating its efficacy in tar cracking and anti-agglomeration. However, dolomite's tendency to fragment at higher temperatures poses a notable challenge [25].

However, agricultural fuel incineration technology is still complex. Furthermore, in the fluidized bed combustion of biomass, the agglomeration of the silica bed material stands out as the predominant operational difficulty linked to ash, especially when burning biomass with a substantial alkali concentration [26]. For these reasons, this work focuses on the combustion of agro-biomass rich with alkali elements at low bed temperatures and the determination of optimal parameters to avoid bed agglomeration. The bed temperature's influence on the formed compounds from agro-biomass combustion were also determined by sampling particulate matter from the FBC.

2. Materials and Methods

2.1. Fuel Selection, Preparation, and Analysis

In the process of developing an experimental biomass fuel combustion bench, different agricultural biomass types were evaluated for their chemical compositions. The bench is designed to burn a range of fuel types, specifically targeting the use of the lowest quality agricultural biomass.

For this biomass comparison, types cited in the scientific literature were used: elephant grass, wheat straw, rice husks, sugarcane fiber, corn, and, particularly, corn cobs. Their ash chemical compositions were sourced from the "Phyllis2" database [27], which lists chemical and physical properties, ash melting temperatures, and other relevant data on various biomass types. For this, Figure 1 presents the composition of different types of biomass originating from agriculture and indicates that corn cobs contain the highest concentration of potassium oxide (K_2O)—these crushed corn cobs were selected as the reference sample with a notably poor composition for combustion tests leading to high-risk ash-related problems.

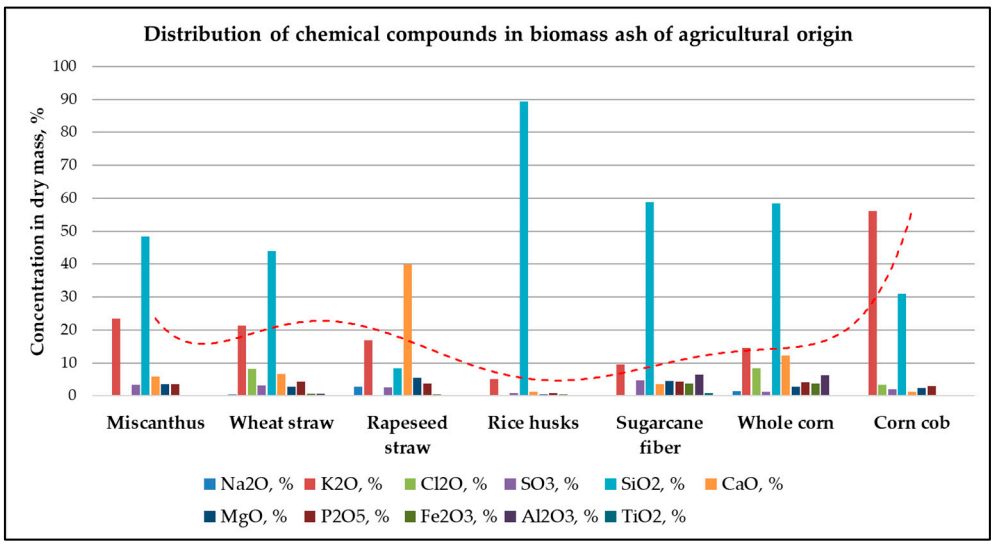

Figure 1. Distribution of chemical compounds in biomass ash of agricultural origin.

The dried corn cob sample was smashed using a Retsch GmbH, SM 300 (Haan, Germany) mill to a fraction of 1 mm. In the following, all tests were carried out with samples of such a fraction. Proximate, ultimate analyses and other physical and chemical parameters of corn cob are given in Table 1. The elemental composition of the corn cob and dolomite, which was used in combustion tests, is given in Table 2. All parameters were determined by an accredited laboratory according to ISO standards. With Binder, FD 115 (Tuttlingen, Germany) furnace total content of moisture of corn cob was performed according to the LST EN ISO 18134-1:2016 standard [28]. Nabertherm GmbH, Muffle Furnace 15/13/P330 (Lilienthal, Germany) was used to determine ash content of corn cob by the LST LT EN ISO 18122:2016 [29] standard. Ion chromatography system Dionex, ICS 5000 (Sunnyvale, United States) was used for sulphur and chlorine determination. Analysis was performed based on LST EN ISO 16994:2016 [30] standard. Main element analyzer ThermoFisher Scientific, Flash 2000 (Waltham, MA, USA) was used for total content of carbon, hydrogen, and nitrogen determination. For this analysis, LST EN ISO 16948:2015 [31] standard was used. Analysis of the chemical elements was performed using inductively coupled plasma with optical emission spectrometer Perkin Elmer, ICP-OES, Optima 8000 (Waltham, MA, USA) device. Major elements were analyzed: Al, Ca, Fe, Mg, P, K, Si, Na, Ti based on LST EN ISO 16967:2015 standard [32]. Minor elements were also analyzed: Zn, Pb, Cr, Cu, Mn based on LST EN ISO 16968:2015 standard. An automatic bomb calorimeter IKA-Werke, IKA C6000 (Staufen, Germany), according to the requirements of the LST EN ISO 18125:2017 [33] standard, was used for calorific value determination. Ash melting behavior was analyzed according to the requirements of ISO 21404:2020(E) standard [34] with Carbolite Gero Ltd., CAF Digital furnace (Shelfield, UK).

Raw material of selected experiment was fully analyzed, and the obtained results were compared with non-specified wood pellets from the literature and databases. The comparison of these materials is necessary to show difference between a well-known fuel as basic with a low-quality fuel.

Table 1. Proximate and ultimate analyses, heating values, and specific ash melting temperatures of corn cobs and non-specified wood pellets.

Parameter	Smashed Corn Cob	Non-Specified Wood Pellets [27,35]
Ultimate analysis		
Carbon, % (d.b)	48.6 ± 0.31	48.90–50.80
Hydrogen, % (d.b)	5.56 ± 0.11	6.17–7.51
Nitrogen, % (d.b)	0.3 ± 0.04	0.03–1.19
Sulphur, % (d.b)	0.3 ± 0.01	0.01–0.1
Oxygen (by difference), % (d.b)	44.29	41.67–44.94
Proximate analysis		
Volatile matter, % (d.b)	81.62 ± 2.11	77.26–83.10
Fixed carbon (calculated), % (d.b)	16.3	16.90–20.39
Ash, % (d.b)	2.07 ± 0.07	0.38–4.60
Moisture (water), %	11.66 ± 0.11	5.20–14.65
HHV, MJ/kg (d.b)	18.86 ± 0.52	20.83–19.47
LHV, MJ/kg (d.b)	17.71 ± 0.57	19.37– 17.22
Specific ash melting temperatures (prepared at 550 °C)		
SST, °C	794 ± 10	1000–1300
DT, °C	802 ± 6	1100–1200
HT, °C	810 ± 4	1160–1350
FT, °C	819 ± 4	1160 → 1350

Table 2. Elemental composition of raw material of corn cob and non-specified wood pellets.

Element	Concentration of Corn Cob, mg/kg	Non-Specified Wood Pellets [35,36]	Concentration of Dolomite, mg/kg
Al	408.88 ± 17.79	4.9–1360	7.12 ± 0.73
Ca	2781.00 ± 249.46	303–16,000	25651.98 ± 502.78
Cr	<0.90	0.083–27	<0.90
Cu	3.86 ± 0.01	0.36–46	0.41 ± 0.0002
Fe	316.76 ± 10.39	9.5–1460	2212.55 ± 100.67
K	6035.85 ± 300.59	167–9833	5502.78 ± 12.66
Mg	291.48 ± 17.02	58–1620	4669.38 ± 153.62
Mn	7.81 ± 1.03	22–702	317.71 ± 9.50
Na	322.32 ± 12.70	8.4–973	386.34 ± 11.01
P	347.91 ± 24.35	22.1–1012	110.13 ± 4.09
Si	5749.60 ± 320.25	115–2694	4.00 ± 0.29
Ti	27.16 ± 1.70	2.65–3.42	7267.67 ± 210.04
Zn	7.63 ± 0.50	1.20–90	108.71 ± 5.21
Pb	10.36 ± 0.89	0.04–11	11.60 ± 0.09

2.2. Experimental Setup and Procedure

Experiments were carried out in a specially designed 500 kW thermal power laboratory stand. The main components are shown in Figure 2, and parameters are presented in Table 3.

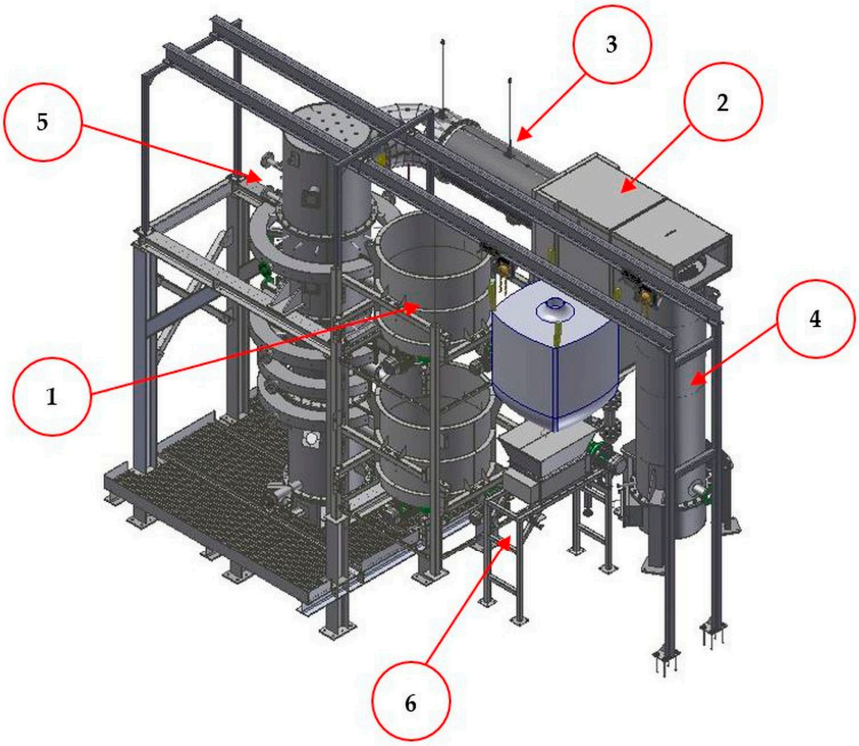

Figure 2. Experimental agro-biomass combustion rig: fuel bunker with feeding auger (1), hot multicyclone (2), specially designed tube section for dust and aerosol sampling (3), heat exchanger for flue gas cooling (4), low-temperature fluidized bed combustion chamber (5), and fuel crusher (6).

Figure 3 shows main fluidized bed reactor parts and locations of installed thermocouples. To keep uniform combustion temperature and initiate fuel self-ignition the lower combustion chamber part was lined with a heat-resistant refractory. Other combustion chamber sections were water-cooled. The thermocouple T_1 was installed directly into the fluidized bed, and other thermocouples (T_2, T_3, T_4, and T_5) were installed at different combustion zone heights. An additional sand was introduced with the dosing auger to maintain a constant fluidized bed height (0.3 m). The fluidized bed height was measured

in accordance with a pressure drop of the bed. Moreover, an additional dosing auger was installed for agglomeration inhibition chemicals. For the experiments with inhibitors, the dolomite was chosen. Elemental analysis of dolomite is presented in Table 2. The supply of dolomite (3% based on fuel supply) was tested at 650 and 700 °C bed temperatures to investigate the effect on agglomeration inhibition.

Table 3. Fluidized bed combustion system parameters.

Parameter	Data
Thermal power	500 kW
FBC height	4.5 m
Bed height	0.3 m
Internal diameter of fluidization area	0.75 m
Internal diameter of combustion chamber	0.85 m
Fluidizing agent	Quartz sand, 0.8–1.0 mm
Fluidizing air distribution plate	19 bubble caps with 5 holes each

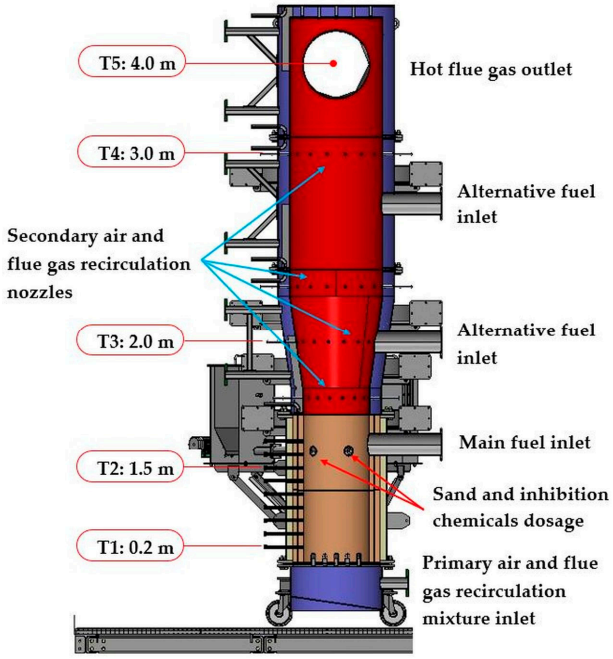

Figure 3. Main parts of fluidized bed reactor.

Before the experiments, the feedstock was prepared: corn cobs were crushed into uniform-sized pieces with a fuel crusher, collected into bags of 1 t, and loaded into a fuel bunker with manual hoisting equipment. Furthermore, the fuel was supplied into the combustion chamber using a speed-controlled auger. Before the combustion experiments, this auger was calibrated with feedstock at different speeds, and the precise amount of fuel was determined. During combustion tests, stable bed fluidization was ensured by supplying the primary air and flue gas mixture at the ~180 m^3/h rate and 4000 Pa pressure. The bed temperature of 650 and 700 °C was controlled by setting the proper flue gas recirculation flow rate and oxygen concentration in the mixed gas flow. In the upper sections, the secondary air was supplied to fully combust generated gases from the fuel. The secondary air flow rates at different heights are controlled with damper to achieve effective combustion process, e.g., to obtain lowest CO and NOx and to control sufficient O_2 concentration in flue gas. From combustion chamber, hot gases at 600–1000 °C go into specially designed tube section for dust and aerosol sampling. This tube is not water-cooled to maintain constant temperature and avoid possible alkali aerosol condensation. In this tube, dust sampling nozzle was mounted.

2.3. Particulate Matter Sampling and Its Chemical Analysis

During the experiments, samples of particulate matter were collected after reaching airflow, biomass feeding, and gaseous emission values at steady-state conditions. During experiment, steady-state conditions were determined and reached after 30–40 min of continuous combustion. When steady-state was achieved, readings were recorded, and particulate matter was taken. After each combustion session, the sand was replaced with new sand. Ten samples of particulate matter were collected from separate areas of boiler, upstream of the cyclone, immediately downstream of the incinerator. Five samples at 650 °C fluidized bed temperature and five at 700 °C fluidized bed temperature were collected. All the samples were ground by ball milling to obtain homogeneous powders. Major (Al, Ca, Fe, Mg, P, K, Si, Na, and Ti) elements and minor (Zn, Pb, Cr, Cu, and Mn) elements in particulate matter from boiler of biomass were determined by ICP-OES.

3. Results and Discussion

3.1. Chemical Composition of Raw Material

The total amount of ash produced during corn cob combustion is composed of volatile fly ashes (fine ash) and non-volatile burnt ashes (coarse ash). The literature analysis shows that non-volatile burnt ashes have a relatively higher melting point and higher volatile matter [37]. Ash content is one indicator of biomass quality. The higher the determined ash content, the lower the heating value (LHV) reached for that kind of biomass [38]. It is seen that corn cobs of this experiment had 2.07 ± 0.07% ash content; meanwhile, in comparison to ash content in wood pellets, it varies from 0.38% to 4.60%. From this view, fuel, such as corn cob, is suitable for direct incineration due to relatively low ash content. In comparison with other investigations [39], the results of the ash content of this study are more than four times lower.

It is known that specific ash melting temperatures are an important parameter of fuel quality. When the ash melting temperatures are better identified, the combustion process can be better optimized, for example, by air supply modifications or by adding different additives to increase the ash melting temperatures [40]. It was determined that the deformation (DT) temperature for low-melting point ashes varies from 1000 to 1200 °C and, for medium-melting point ashes, it varies from 1200 to 1450 °C. For high-melting point ashes, the deformation (DT) temperature is over 1450 °C. It was determined that during the combustion of woody biomass, the temperature of 1100 °C should not be exceeded [41]. From the obtained results (Table 1), it is seen that all analyzed wood pellets have a deformation temperature no lower than 1100 °C. An analysis of the corn cobs used in this study by ash melting classification showed a very low melting point at all melting stages (ST, DT, HT, FT). Corn cob ash deformation starts at 802 °C and fully melts at 819 °C. Similar results were found in [40]; ashes produced from corn cobs had deformation temperatures below 1000 °C. The difference between the melting process initiation and the ending was determined at just 17 °C. The severity of ash melting problems largely depends on the fractions of alkali metals, especially K, alkaline earth metal (Mg, Ca), and other inorganic elements (i.e., Cl, S, and Si) distribution. Alkali group metals in high-alkali fuels can be categorized into two groups: easily volatile metals and less volatile metals (silicates, alum inosilicates). The results of corn cobs and wood pellets in comparison to chemical elements are prepared in Table 2.

An analysis showed that corn cobs have the highest concentrations of Si, Ti, and Pb in comparison to non-specified wood pellets. Silicon content was found to be more than two times and titanium content to be more than seven times greater than the highest concentrations of wood pellets. Also, the lead concentration was found to be quite high in corn cob: 10.36 ± 0.89 mg/kg. It was determined that with the higher chlorine or sulphur, silica, and alkali content in biomass fuels, the exit flue gas high temperature of such fuel promotes slagging and deposition processes on boiler surfaces [42]. The variation of Ca, K, and Na in wood pellets from the literature was found in a wide range. It is directly influenced by raw material quality. From the obtained data, it is seen that corn cobs

have a high amount of potassium; the concentration was 6035.85 ± 300.59 mg/kg. The composition of the ash samples is presented in Table 4. The percentage of main element oxides varied owing to the contrasting origins of corn cobs and wood pellets. The main constituents of corn cob ash were K_2O—56.03% and SiO_2—31.02%. The same distribution of K_2O and SiO_2 was in [43]; respectively, it was determined from 23.4% to 58.11% and from 13.4% to 37.58%. The presence of alkaline oxide in large amounts within the ash content plays a crucial role in the uninterrupted operation of a biomass gasifier or combustor [44]. The risk involves their ability to reduce the ash's melting point and their tendency to vaporize at the temperatures found within a biomass gasifier/combustor, followed by condensation on cooler surfaces [45]. Other element oxides were found just in the range of 1–4% or less of the total ash composition. Different distribution of the mentioned element oxides is presented in wood pellet ashes. In wood pellet ash, the highest amount of CaO, SiO_2, and MgO was found.

Table 4. ICP-OES analysis of corn cob ashes (% by weight) fully combusted at 550 °C and non-specified wood pellets.

Element	Part by Weight of Corn Cob Ash, %	Part by Weight of Wood Pellet Ash [35,46], %
Al_2O_3	0.33	1.66–283
CaO	1.20	25.18–56.28
Fe_2O_3	0.37	2.11–3.67
MgO	2.32	4.58–8.72
P_2O_5	3.07	0.22–4.68
K_2O	56.03	2.68–17.18
SiO_2	31.02	4.75–30.31
Na_2O	0.05	0.63–1.09
TiO_2	0.01	<0.01–0.29
ZnO	0.26	<0.05
PbO	0.0004	<0.01

3.2. Combustion Tests of FBC and Optimal Parameters

The first set of experiments was performed to determine parameters to achieve stable and efficient combustion for two bed temperatures: 650 °C and 700 °C. The bed temperature was selected according to feedstock ash melting temperature (Table 1) and to avoid fuel agglomeration in the fluidized bed. The bed temperature was controlled by changing the primary air (PA) and flue gas recirculation (FGR) proportion supplied to the bed, and different tests with various FGR/PA ratios (see Table 5) were performed at the desired fluidized bed temperature to maintain a stable bed temperature and combustion process without fluctuations. During the experiments, it was determined that the stable bed temperature of 650 °C is ensured by changing the FGR/PA ratio from 0.42 to 0.65, but at higher PA/FGR ratios, CO emissions increased by 200–500 mg/m^3, even adjusting secondary air (SA) staging to the combustion zones. It was found that the SA and FGR/PA ratio has to be adjusted to maintain 3.3–3.8% of O_2 concentration in flue gases and 10–11% of O_2 in PA/FGR mixture to maintain a stable bed temperature of 650 °C with sufficient oxygen concentration in the mixed gas flow supplied to the bed. At higher ratios of FGR/PA (from 0.55 to 0.65), the increased amount of FGR resulted in a cooling effect, which, in turn, caused insufficient combustion, and secondary air staging had no effect on an improvement of combustion performance. It was caused due to decreased chamber temperature which was not sufficient for ignition of formed combustible gases in the fluidized bed area. Meanwhile, an opposite effect was obtained at too low FGR/PA ratios as the excess oxygen concentration in FGR leads to higher bed temperature and without adjustment of FGR amount, the bed could exceed 700 °C.

Table 5. Parameters of combustion tests at different fluidized bed temperatures.

Bed Temperature	**650 °C**				**700 °C**			
Fuel amount, kg/h	~132				~132			
Thermal power, kW	~500				~500			
Supply of PA and FGR mixture, m^3/h	180				180			
T2, °C	690	689	715	705	734	756	803	744
T3, °C	986	981	1014	989	1005	1008	1014	995
T4, °C	752	778	740	733	756	754	726	692
T5, °C	830	865	805	800	873	889	819	829
Ratio of PA/FGR	0.42	0.49	0.58	0.65	0.22	0.33	0.38	0.44
Secondary air, m^3/h	656	911	954	717	603	642	667	658
SA to zone I, %	34	25	29	31	19	20	33	30
SA to zone II, %	42	32	27	39	26	28	20	28
SA to zone III, %	5	4	3	4	13	15	1	3
SA to zone IV, %	43	39	41	40	42	38	46	49
O_2 concentration in flue gas, %	3.1	3.3	3.8	4.1	2.27	2.98	3.5	3.1
O_2 concentration in PA/FGR mixture, %	10.4	10	10.4	10.4	12.6	11.9	12.6	10.2
Air equivalence ratio	1.17	1.19	1.22	1.24	1.12	1.17	1.2	1.17
CO, mg/m^3	1168	1354	1402	1468	693	1018	971	748
NOx, mg/m^3	379	222	285	289	426	323	333	343

In the case of a bed temperature of 700 °C, corrections of the PA/FGR ratio and SA staging to the combustion zones were carried out as well (see Table 5). Compared to the combustion mode at the 650 °C bed temperature, the higher temperature combustion mode required a higher proportion of primary air. To determine optimal parameters of FBC mode at the bed temperature of 700 °C different tests changing FGR/PA ratio from 0.22 to 0.44 were performed. Independently of the FGR/PA ratio, achieved CO concentrations in the flue gas were lower due to the increased temperature in the combustion chamber, but it affected NOx concentrations negatively (see Table 5).

According to performed tests, the optimal parameters in terms of stable combustion temperature and lowest CO and NOx emissions were achieved, maintaining the FGR/PA ratio in the range of 0.22–0.33. Also, tests revealed that the SA and FGR/PA ratio has to be adjusted to maintain 2.3–3.5% of O_2 concentration in flue gases and 10–12% of O_2 in PA/FGR mixture to maintain a stable bed temperature of 700 °C. The secondary air staging has a low effect on NOx but influenced combustion efficiency as better CO combustion was achieved. The optimal parameters of both temperature modes are presented in Table 6. Based on these parameters, additional tests with added dolomite were performed. Below is the determined temperature profile for the different bed temperatures with and without the addition of dolomite (see Figure 4). Due to the supplement of PA/FGR mixture to the fluidized bed layer, an insufficient amount of oxygen and a high amount of CO_2 causes incomplete combustion of fuel, leading to a controllable low temperature of the bed (650 °C and 700 °C), and the released combustible gases are ignited about 1.5 m over the fluidized bed. At this zone, the highest amount of SA is supplied, and the temperature increases up to ~980 °C and ~1015 °C, respectively, for cases of 650 °C and 700 °C bed temperatures. In upper combustion zones, the temperature drops, and the SA amount is controlled to keep the autoignition temperature of CO. In the case of added dolomite, the bed temperature started to increase, and the PA/FGR ratio was changed by decreasing the primary air amount in the mixture (Table 6) in both cases. Despite that, slightly higher temperatures were registered in the FCB. In the case of 650 °C, the temperature increased by 15 °C over the fluidized bed and by 20–30 °C in the third and fourth combustion zones. A slightly different

trend was obtained at higher bed temperature (700 °C). The highest temperature increase was determined in the fluidized bed area, by 35 °C at the T_2 point; even the PA/FGR ratio was corrected. This effect could be caused by a higher bed temperature leading to more intense reactions promoted by dolomite. Dolomite is characterized by its ability to adsorb substances on its surface, filter them through its pores, and facilitate ion exchange among its ore layers. The temperature increase in the layer is influenced by the decomposition of $MgCO_3$ and $CaCO_3$ from dolomite into MgO and CaO [47]. According to Chi et al. [48], it was found that during the combustion of wheat straw, the bed temperature increased from 870 °C to 900 °C due to added dolomite. The determined optimal parameters of the FBC are presented in Table 2. Need to point out that during tests at both bed temperatures, the defluidization effect was not observed over 8–10 working hours per run due to low bed temperatures and intense mixing of fuel particles and sand particles (>1 m/s flow per bed layer) [49].

Table 6. Optimal parameters of the fluidized bed combustor.

Bed Temperature	**650 °C**		**700 °C**	
Condition	**W/O Dolomite**	**With Dolomite**	**W/O Dolomite**	**With Dolomite**
Fuel amount, kg/h	132			
Thermal power, kW	~500			
Dolomite amount, kg/h	0	~3.9	0	~3.9
Supply of PA and FGR mixture, m^3/h	180			
Ratio of FGR/PA	0.51	0.42	0.22	0.24
Secondary air, m^3/h	736	769	658	667
SA to zone I, %	25	29	19	20
SA to zone II, %	32	36	26	27
SA to zone III, %	4	4	13	14
SA to zone IV, %	40	37	42	38
O_2 concentration in flue gas, %	3.4	4.1	2.27	2.32
O_2 concentration in PA/FGR mixture, %	10.1	10.4	12.6	11.9
Air equivalence ratio	1.19	1.24	1.12	1.12

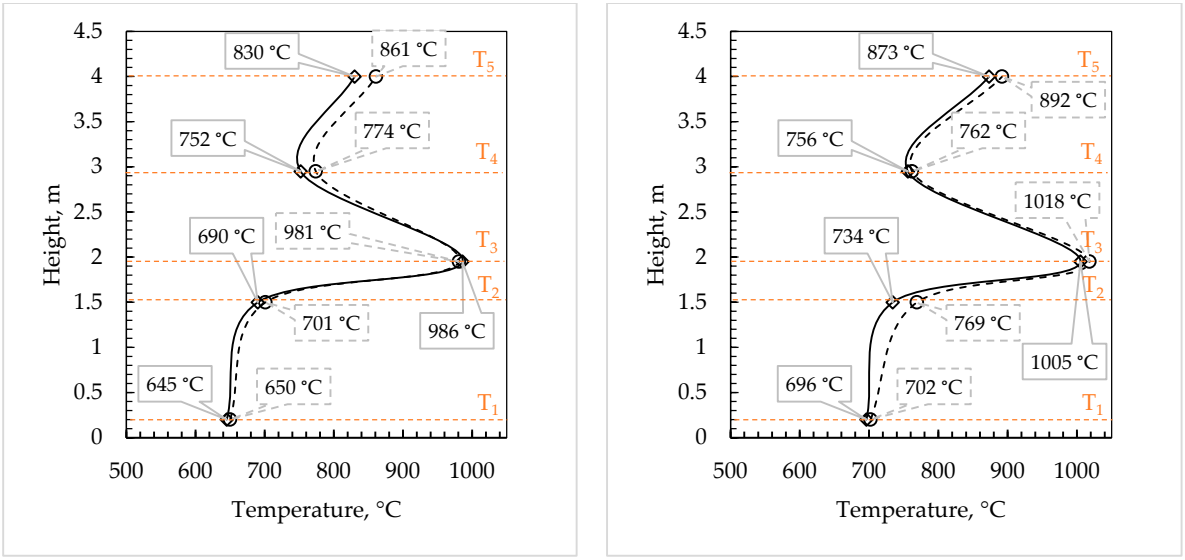

(**a**) (**b**)

Figure 4. Temperature profile in the FBC at fluidization temperatures of (**a**) 650 °C, (**b**) 700 °C without additive (solid line), and with 3% of dolomite (dashed line).

3.3. Pollutant Emissions during Combustion at Different Fluidized Bed Temperatures

During combustion tests under determined optimal conditions (Table 6), the concentrations of pollutant emissions (CO, NOx, OGC, SO_2) and particulate matter (PM) in flue gas at the FBC exit were measured at fluidized bed temperature of 650 °C and 700 °C. Also, the influence of the additive (3% dolomite) supplied with the fuel on the emission concentrations was determined. The concentrations of emissions were presented as mass concentrations, calibrated to dry flue gas conditions at a 6% oxygen level, and set to standard conditions at 0 °C and 1013 mbar (Figure 5).

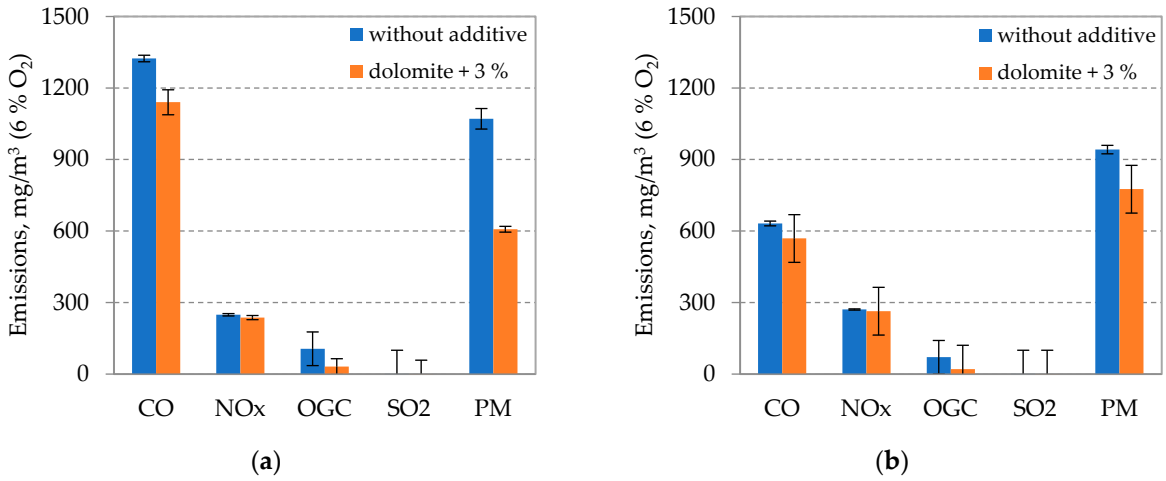

Figure 5. Emissions in flue gas at different fluidized bed temperatures: (**a**) 650 °C; (**b**) 700 °C.

As the bed temperature rises, the efficiency of combustion improves, leading to a decrease in the levels of unburned particles and CO within the flue gas [50]. Increasing the fluidized bed temperature from 650 °C to 700 °C decreased the CO emissions by approximately 50%. Maintaining the same bed temperature results in an increased temperature in the combustion zone because of the reduced temperature gradient, which improves the efficiency of gas generated from burning fuel, thereby leading to a decrease in CO emissions. NOx emissions increased by ~9%, but OGC and PM emissions decreased by 33% and 12%, respectively. The NOx and OGC emissions were determined in relatively low concentrations due to longer residence time for the combusting particles in the fluidized bed combustor. The increase in bed temperature also encourages the creation of NH3 and HCN, crucial precursors to NO, leading to enhanced NO emissions [51]. The concentration of SO_2 emission in both cases was determined to be less than 1 mg/m^3. At a fluidized bed temperature set to 750 °C, an augmentation in the primary air volume leads to a decline in SO_2 emissions, largely attributed to the increased presence of oxygen in the combustor, which aids in the self-desulfurization capacity of char [50].

A benefit of 3% added dolomite on combustion quality was observed in both temperature regimes. Comparing the influence of the additive at different temperatures, it was observed that at a fluidized bed temperature of 650 °C, CO, OGC, and PM emissions decreased by 14%, 70%, and 43%, respectively. Keeping the fluidized bed temperature at 700 °C resulted in similar reductions in CO, OGC, and PM emissions by 10%, 70%, and 17%. A higher temperature of the fluidized bed had the opposite effect on the concentration of NOx. As the temperature increased, the effect of the additive on NOx emissions decreased from 4.8% to 2.5%. SO_2 emissions were not detected when the dolomite additive was used.

3.4. Release of Chemical Elements from Fuel during Combustion at Different Fluidized Bed Temperatures Using an Inhibitor

During the burning process, assorted mineral elements undergo precipitation at separate stages, which plays a role in the development of PM of various dimensions [52]. The released elemental concentrations in particulate matter in percentage under different

combustion conditions are presented in Figure 6. Results are shown as element differences in % from feedstock (100%). The comparison of element exchange in PM was analyzed under two boiler working conditions: 650 °C and 700 °C. The results can be divided into three different categories, regardless of whether or not an additive was added: (1) a high exchange of elements in PM (Mg, Cu, Si, Ca); (2) a medium exchange of elements in PM (Zn, Mn, K, Al); and (3) a low exchange of elements in PM (P, Na, Fe). It should be noted that Cr, Ti, Zn, and Pb in PM were not found in both conditions of the test.

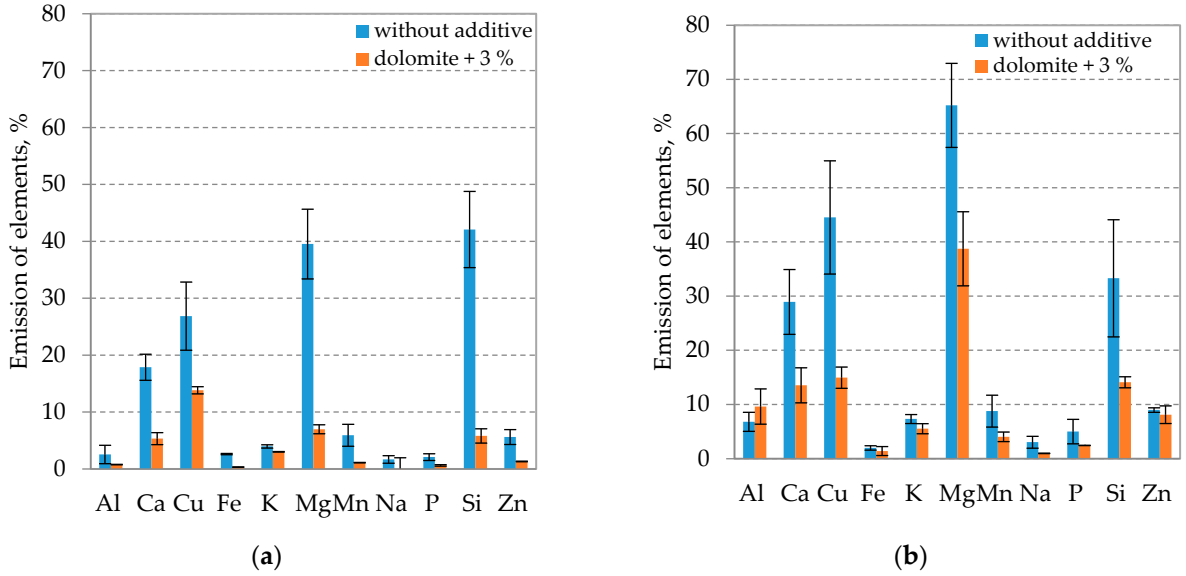

Figure 6. Element amount exchange in particulate matter at different fluidized bed temperatures: (**a**) 650 °C; (**b**) 700 °C.

Under 650 °C boiler working conditions without additive Mg, about 39.5%, Cu—29%, Si—42%, and Ca—18% were realized. Under 700 °C boiler working conditions without additive Mg, about 65%, Cu—44%, Si—33%, and Ca—28% were realized. With an increasing combustion zone temperature, Ca, Cu, and Mg exchange increased significantly, but silicon exchange decreased. Studies and thermodynamic predictions demonstrate that with an increase in combustion temperature, potassium reacts with silicon to produce potassium silicates, which contribute to slagging by adhering to silicon [38]. The lowest silicon exchange in the 700 °C combustion zone shows that silicon was bound in bottom ash, possibly in conjunction with potassium salts. Other element exchange increasing combustion temperature from 650 °C to 700 °C also increased, but the exception was determined for Fe. With an increase in combustion temperature, there is a modest decrease in the Fe exchange within particulate matter, dropping from 2.62% to 1.99%. This phenomenon may be influenced by the increased rates of evaporation and condensation of mineral elements at higher temperatures [52].

The additives' influence in realizing the content of elements in PM is obvious. The decrease was found for all analyzed elements, except aluminum; the amount of Al slightly increased at a 700 °C boiler operating temperature. Obtained results showed that the highest realization from fuel was determined to be Mg, Cu, Si, and Ca in PM. The highest exchange, under 650 °C boiler working conditions, Mg and Si elements were found. Dolomite additive decreased these elements, respectively, by 32% and 36% in PM in comparison with the incineration process without an additive. The highest exchange, under 700 °C boiler working conditions, Ca and Cu elements were found. Dolomite additive decreased these elements, respectively, 15% and 29.5% in PM in comparison with the incineration process without additive. Other elements decrease under the addition of dolomite was found in a lower range. Medium exchange elements Zn, Mn, K, and Al were found in 650 °C boiler working conditions, respectively, from 4.81% to 0.95, and in 700 °C boiler working

conditions, from 4.75% to 0.86%. The same situation with low exchange elements P, Na, and Fe was determined in PM. In 650 °C boiler working conditions, P, Na, and Fe decreased, respectively, from 2.28% to 1.45%, and in 700 °C boiler working conditions, from 2.55% to 0.59%. The decrease in selected elements was found due to dolomite promoting the formation of high-melting point minerals such as magnesium silicate ($MgO:XSiO_2 \bullet H_2O$), periclase (MgO), orthoclase ($KAlSi_3O_8$), $CaMgSi_2O6$ and wollastonite ($CaSiO_3$) in ash, reduces the liquid phase and controls the growth of ash adhesion strength [22]. The biggest part of the element is left in ashes.

4. Conclusions

The experimental investigation of corn cob combustion at low temperatures was performed in a specially design fluidized bed combustor, and its performance was tested under 500 kW thermal power. During the tests, optimal parameters were established and determined that the optimal air equivalence ratio should be 1.15–1.24 depending on the bed temperature, and the bed temperature is controlled by adjusting the primary air and flue gas mixture ratio as the overall flow should be maintained constant to ensure sufficient fluidization velocity. During the combustion process, when the excess air coefficient reaches 1.3–1.4, higher oxygen concentrations (5–6%) are formed in the flue gas, and corrections of the PA and FGR ratio in the mixture is required (the amount of primary air is reduced) to maintain a 10–12% oxygen concentration in the mixture and to maintain a stable temperature of the fluidized bed. However, when supplying the PA/FGR mixture of the above composition, the combustion chamber is cooled more intensively, and it is difficult to maintain a stable combustion process. Pulsations appear, and CO concentrations increase.

It was found that the bed temperature of 650 °C leads to higher CO emissions by about 50% compared to 700 °C. However, the addition of dolomite led to improved combustion efficiency, and CO, OGC, and PM emissions decreased by 14%, 70%, and 43%, respectively. Keeping the fluidized bed temperature at 700 °C resulted in similar reductions in CO, OGC, and PM emissions by 10%, 70%, and 17%.

Adding dolomite acts to impede the melting of potassium and ensures its incorporation into the ash, facilitating the creation of compounds with elevated melting points. The decomposition of $MgCO_3$ and $CaCO_3$ within dolomite leads to an increased presence of high-melting-point minerals in the ash. By incorporating dolomite, ash is enriched with thermally stable minerals, including orthoclase ($KAlSi_3O_8$), $CaMgSi_2O_6$, wollastonite ($CaSiO_3$), periclase (MgO), and magnesium silicate ($MgO:XSiO_2 \bullet H_2O$). Dolomite plays a crucial role in inhibiting silicate melting, reducing the formation of a liquid phase, and decreasing both the adhesive properties and the emission of chemical elements with particulate matter in corn cob fly ashes. It was found that the bed temperature of 650 °C leads to a decrease in high exchange elements (Mg, Cu, Si, Ca) in a range from 12% to 36%, and 700 °C leads to a decrease in a range from 15% to 29%.

During extended experiments lasting 8 h, no agglomeration of the fluidized bed was observed. Moreover, the proposed configuration of the FBC and its operational parameters prove suitable for facilitating the efficient combustion of agricultural biomass.

Author Contributions: Conceptualization, R.P. and M.P.; methodology, I.A. and K.Z.; software, M.P. and E.L.; validation, R.P., M.P. and K.Z.; formal analysis, R.P., I.A., M.P. and E.L.; investigation, R.P., M.P., I.A., K.Z. and J.E.; resources, I.A. and N.S.; data curation, J.E.; writing—original draft preparation, R.P., M.P., E.L. and I.A.; writing—review and editing, R.P. and M.P.; visualization, K.Z. and J.E.; supervision, R.P.; project administration, I.A.; funding acquisition, R.P. and N.S. All authors have read and agreed to the published version of the manuscript.

Funding: This research received no external funding.

Data Availability Statement: Dataset available on request from the authors.

Conflicts of Interest: The authors declare no conflicts of interest.

Abbreviations

FBC	fluidized bed combustor
RES	renewable energy sources
HHV	higher heating value, MJ/kg
LHV	lower heating value, MJ/kg
SST	shrinkage starting temperature, °C
DT	deformation temperature, °C
HT	hemisphere temperature, °C
FT	flow temperature, °C
PA	primary air, m^3/h
SA	secondary air, m^3/h
FGR	flue gas recirculation, m^3/h
OGC	organic gaseous compounds, mg/m^3
PM	particulate matter, mg/m^3

References

1. Saleem, M. Possibility of utilizing agriculture biomass as a renewable and sustainable future energy source. *Heliyon* **2022**, *8*, e08905. [CrossRef]
2. Janiszewska, D.; Ossowska, L. The Role of Agricultural Biomass as a Renewable Energy Source in European Union Countries. *Energies* **2022**, *15*, 6756. [CrossRef]
3. Krishna Koundinya, K.; Dobhal, P.; Ahmad, T.; Mondal, S.; Kumar Sharma, A.; Kumar Singh, V. A technical review on thermochemical pathways for production of energy from corncob residue. *Renew. Energy Focus* **2023**, *44*, 174–185. [CrossRef]
4. Choi, J.Y.; Nam, J.; Yun, B.Y.; Kim, Y.U.; Kim, S. Utilization of corn cob, an essential agricultuaral residue difficult to disposal: Composite board manufactured improved thermal performance using microencapsulated PCM. *Ind. Crops Prod.* **2022**, *183*, 114931. [CrossRef]
5. Gani, A.; Reza, M.; Desvita, H. Proximate and ultimate analysis of corncob biomass waste as raw material for biocoke fuel production. *Case Stud. Chem. Environ. Eng.* **2023**, *8*, 100525. [CrossRef]
6. Honorato-Salazar, J.A.; Sadhukhan, J. Annual biomass variation of agriculture crops and forestry residues, and seasonality of crop residues for energy production in Mexico. *Food Bioprod. Process.* **2020**, *119*, 1–19. [CrossRef]
7. Donskoy, I. Particle Agglomeration of Biomass and Plastic Waste during Their Thermochemical Fixed-Bed Conversion. *Energies* **2023**, *16*, 4589. [CrossRef]
8. Shao, Y.; Wang, J.; Preto, F.; Zhu, J.; Xu, C. Ash deposition in biomass combustion or co-firing for power/heat generation. *Energies* **2012**, *5*, 5171–5189. [CrossRef]
9. Johansen, J.M.; Jakobsen, J.G.; Frandsen, F.J.; Glarborg, P. Release of K, Cl, and S during Pyrolysis and Combustion of High-Chlorine Biomass. *Energy Fuels* **2011**, *25*, 4961–4971. [CrossRef]
10. Alam, T.; Hoadley, A.; Dai, B.; Zhang, L. Impact of potassium on bio-ash slagging and resultant slag flowing characteristics under mild reducing environment. *Fuel Process. Technol.* **2023**, *243*, 107672. [CrossRef]
11. Mlonka-Mędrala, A.; Magdziarz, A.; Gajek, M.; Nowińska, K.; Nowak, W. Alkali metals association in biomass and their impact on ash melting behaviour. *Fuel* **2020**, *261*, 116421. [CrossRef]
12. Leckner, B.; Szentannai, P.; Winter, F. Scale-up of fluidized-bed combustion—A review. *Fuel* **2011**, *90*, 2951–2964. [CrossRef]
13. Yoon, S.H.; Kim, S.-J.; Baek, G.-U.; Moon, J.H.; Jo, S.H.; Park, S.J.; Kim, J.-Y.; Yoon, S.-J.; Ra, H.W.; Yoon, S.-M.; et al. Operational optimization of air staging and flue gas recirculation for NOx reduction in biomass circulating fluidized bed combustion. *J. Clean. Prod.* **2023**, *387*, 135878. [CrossRef]
14. Peng, T.-H.; Lin, C.-L.; Wey, M.-Y. Development of a low-temperature two-stage fluidized bed incinerator for controlling heavy-metal emission in flue gases. *Appl. Therm. Eng.* **2014**, *62*, 706–713. [CrossRef]
15. Thomsen, T.P.; Hauggaard-Nielsen, H.; Gøbel, B.; Stoholm, P.; Ahrenfeldt, J.; Henriksen, U.B.; Müller-Stöver, D.S. Low temperature circulating fluidized bed gasification and co-gasification of municipal sewage sludge. Part 2: Evaluation of ash materials as phosphorus fertilizer. *Waste Manag.* **2017**, *66*, 145–154. [CrossRef]
16. Thomsen, T.P.; Sárossy, Z.; Gøbel, B.; Stoholm, P.; Ahrenfeldt, J.; Frandsen, F.J.; Henriksen, U.B. Low temperature circulating fluidized bed gasification and co-gasification of municipal sewage sludge. Part 1: Process performance and gas product characterization. *Waste Manag.* **2017**, *66*, 123–133. [CrossRef]
17. Karel, T.; Fürsatz, K.; Priscak, J.; Kuba, M.; Skoglund, N.; Hofbauer, H. Influence of fuel characteristics of alternative residual biomass and ash chemistry on fluidized bed combustion and gasification. *Energy* **2020**, *219*, 119650.
18. Silvennoinen, J.; Hedman, M. Co-firing of agricultural fuels in a full-scale fluidized bed boiler. *Fuel Process. Technol.* **2013**, *105*, 11–19. [CrossRef]
19. Saastamoinen, H.; Leino, T. Fuel Staging and Air Staging To Reduce Nitrogen Emission in the CFB Combustion of Bark and Coal. *Energy Fuels* **2019**, *33*, 5732–5739. [CrossRef]

20. Chyang, C.-S.; Qian, F.-P.; Lin, Y.-C.; Yang, S.-H. NO and N_2O Emission Characteristics from a Pilot Scale Vortexing Fluidized Bed Combustor Firing Different Fuels. *Energy Fuels* **2008**, *22*, 1004–1011. [CrossRef]
21. Hariana; Prismantoko, A.; Prabowo; Hilmawan, E.; Darmawan, A.; Aziz, M. Effectiveness of different additives on slagging and fouling tendencies of blended coal. *J. Energy Inst.* **2023**, *107*, 101192. [CrossRef]
22. Liu, Z.; Jin, J.; Zheng, L.; Zhang, R.; Dong, B.; Liang, G.; Zhai, Z. Adhesion strength of straw biomass ash: Effect of dolomite additive. *Energy* **2023**, *262*, 125320. [CrossRef]
23. Maj, I.; Matus, K. Aluminosilicate Clay Minerals: Kaolin, Bentonite, and Halloysite as Fuel Additives for Thermal Conversion of Biomass and Waste. *Energies* **2023**, *16*, 4359. [CrossRef]
24. Benny, M.; Suraj, P.; Arun, P.; Muraleedharan, C. Agglomeration behavior of lignocellulosic biomasses in fluidized bed gasification: A comprehensive review. *J. Therm. Anal. Calorim.* **2023**, *148*, 9289–9308. [CrossRef]
25. Hervy, M.; Olcese, R.; Bettahar, M.M.; Mallet, M.; Renard, A.; Maldonado, L.; Remy, D.; Mauviel, G.; Dufour, A. Evolution of dolomite composition and reactivity during biomass gasification. *Appl. Catal. A Gen.* **2019**, *572*, 97–106. [CrossRef]
26. Çelikler, C.; Varol, M. Investigation of control methods for agglomeration and slagging during combustion of olive cake in a bubbling fluidized bed combustor. *J. Clean. Prod.* **2021**, *320*, 128841. [CrossRef]
27. TNO Biobased and Circular Technologies Phyllis2, Database for (Treated) Biomass, Algae, Feedstocks for Biogas Production and Biochar. Available online: https://phyllis.nl/ (accessed on 4 April 2024).
28. *ISO 18134-1:2016*; LST EN. ISO Tarptautinė Standartizacijos Organizacija: Geneva, Switzerland. Available online: https://eshop.lsd.lt/public#!/product/info/0a640308-84af-17ba-8184-c3c1fbec00ea (accessed on 4 April 2024).
29. *ISO 18122:2016*; Standartizacijos LST LT EN. ISO Tarptautinė Standartizacijos Organizacija: Geneva, Switzerland. Available online: https://eshop.lsd.lt/public#!/product/info/0a64031d-8211-1029-8184-762685b30677 (accessed on 4 April 2024).
30. *ISO 16994:2016*; Standartizacijos LST EN. ISO Tarptautinė Standartizacijos Organizacija: Geneva, Switzerland. Available online: https://eshop.lsd.lt/public#!/product/info/0a640324-6747-1da0-8168-815006b5174d (accessed on 4 April 2024).
31. *ISO 16948:2015*; Standartizacijos LST EN. ISO Tarptautinė Standartizacijos Organizacija: Geneva, Switzerland. Available online: https://eshop.lsd.lt/public#!/product/info/0a640324-6747-1da0-8168-8adfadca1c24 (accessed on 4 April 2024).
32. *ISO 16967:2015*; Standartizacijos LST EN. ISO Tarptautinė Standartizacijos Organizacija: Geneva, Switzerland. Available online: https://eshop.lsd.lt/public#!/product/info/0a640324-6747-1da0-8168-8adfadc81c1d (accessed on 4 April 2024).
33. *ISO 18125:2017*; Standartizacijos LST EN. ISO Tarptautinė Standartizacijos Organizacija: Geneva, Switzerland. Available online: https://eshop.lsd.lt/public#!/product/info/0a640324-6747-1da0-8168-7c8308020f6d (accessed on 4 April 2024).
34. *ISO 21404:2020*; Standartizacijos. ISO Tarptautinė Standartizacijos Organizacija: Geneva, Switzerland. Available online: https://eshop.lsd.lt/public#!/product/info/0a640325-6f72-19c7-816f-f758e2d2014c, (accessed on 4 April 2024).
35. BIODAT Database. Available online: https://biodat.eu/pages/Search.aspx (accessed on 9 April 2024).
36. Chandrasekaran, S.R.; Hopke, P.K.; Rector, L.; Allen, G.; Lin, L. Chemical Composition of Wood Chips and Wood Pellets. *Energy Fuels* **2013**, *26*, 4932–4937. [CrossRef]
37. Zhai, M.; Li, X.; Yang, D.; Ma, Z.; Dong, P. Ash fusion characteristics of biomass pellets during combustion. *J. Clean. Prod.* **2022**, *336*, 130361. [CrossRef]
38. Rodríguez, J.L.; Álvarez, X.; Valero, E.; Ortiz, L.; de la Torre-Rodríguez, N.; Acuña-Alonso, C. Influence of ashes in the use of forest biomass as source of energy. *Fuel* **2021**, *283*, 119256. [CrossRef]
39. Zając, G.; Szyszlak-Bargłowicz, J.; Gołębiowski, W.; Szczepanik, M. Chemical characteristics of biomass ashes. *Energies* **2018**, *11*, 2885. [CrossRef]
40. Čajová Kantová, N.; Holubčík, M.; Trnka, J.; Čaja, A. Analysis of Ash Melting Temperatures of Agricultural Pellets Detected during Different Conditions. *Fire* **2023**, *6*, 88. [CrossRef]
41. Radačovská, L.; Holubčík, M.; Nosek, R.; Jandačka, J. Influence of Bark Content on Ash Melting Temperature. *Procedia Eng.* **2017**, *192*, 759–764. [CrossRef]
42. Sun, P.; Wang, C.; Zhang, M.; Cui, L.; Dong, Y. Ash problems and prevention measures in power plants burning high alkali fuel: Brief review and future perspectives. *Sci. Total Environ.* **2023**, *901*, 165985. [CrossRef] [PubMed]
43. Al-Qayim, K.; Nimmo, W.; Hughe, K.J.; Pourkashanian, M. Effect of oxy-fuel combustion on ash deposition of pulverized wood pellets. *Biofuel Res. J.* **2019**, *6*, 927–936. [CrossRef]
44. Miranda, M.T.; García-Mateos, R.; Arranz, J.I.; Sepúlveda, F.J.; Romero, P.; Botet-Jiménez, A. Selective use of corn crop residues: Energy viability. *Appl. Sci.* **2021**, *11*, 3284. [CrossRef]
45. Yao, X.; Hu, Y.; Ge, J.; Ma, X.; Mao, J.; Sun, L.; Xu, K.; Xu, K. A comprehensive study on influence of operating parameters on agglomeration of ashes during biomass gasification in a laboratory-scale gasification system. *Fuel* **2020**, *276*, 118083. [CrossRef]
46. Quoc Viet, D.; Van Vinh, N.; Luong, P.H.; Dinh, V.; Tho, S. Thermogravimetric Study on Rice, Corn and Sugar Cane Crop Residue. *J. Sustain. Energy Environ.* **2015**, *6*, 87–91.
47. Zheng, L.; Jin, J.; Zhang, R.; Liu, Z.; Zhang, L. Understanding the effect of dolomite additive on corrosion characteristics of straw biomass ash through experiment study and molecular dynamics calculations. *Energy* **2023**, *271*, 126950. [CrossRef]
48. Chi, H.; Pans, M.A.; Sun, C.; Liu, H. Effectiveness of bed additives in abating agglomeration during biomass air/oxy combustion in a fluidised bed combustor. *Renew. Energy* **2022**, *185*, 945–958. [CrossRef]
49. Duan, F.; Chyang, C.-S.; Zhang, L.; Yin, S.-F. Bed agglomeration characteristics of rice straw combustion in a vortexing fluidized-bed combustor. *Bioresour. Technol.* **2015**, *183*, 195–202. [CrossRef]

50. Li, L.; Mao, J.; Tang, W.; Sun, G.; Gu, Q.; Lu, X.; Shao, K.; Chen, Y.; Duan, L. Experimental study on coal combustion by using the ilmenite ore as active bed material in a 0.3 MWth circulating fluidized bed. *Fuel* **2023**, *342*, 127007. [CrossRef]
51. Schmid, D.; Karlström, O.; Yrjas, P. Release of NH_3, HCN and NO during devolatilization and combustion of washed and torrefied biomass. *Fuel* **2020**, *280*, 118583. [CrossRef]
52. Sun, Q.; Zhao, Z.; Wang, S.; Zhang, Y.; Da, Y.; Dong, H.; Wen, J.; Du, Q.; Gao, J. Effects of Temperature and Chemical Speciation of Mineral Elements on PM10 Formation during Zhundong Coal Combustion. *Energies* **2022**, *16*, 310. [CrossRef]